International Journal for Multidisciplinary Research (IJFMR)
E-ISSN: 2582-2160 ● Website: www.ijfmr.com ● Email: editor@ijfmr.com

A Comparative Study of Synthesis and Characterization of Pure and Dual Doped (Cu-Co)α-MnO_2 Nanorods

S. Kirtuhika[1*], K. Ramesh[2], G. Viruthagiri[3], T.Thilagavathi[4]

[1]Research Scholar, Department of Physics, Goverenment Arts College, C Mutlur, Chidambaram 608102, Tamilnadu, India
[1]Assistant professor, Department of Physics, Goverenment Arts College, C Mutlur, Chidambaram 608102, Tamilnadu, India
[3]Associate Professor, Department of Physics, Thiru Kolanjiappar Government Arts College, Virudhachalam-606 001, Tamilnadu, India
[4]Assistant Professor**,** Department of Physics Government College for Women(A),Kumbakonam - 612001, Tamilnadu, India

Abstract:
In this study synthesized manganese oxide (α-MnO_2) nanoparticles with dual doping of cobalt (Co) and copper (Cu) nanorods. We investigated optimal conditions in Cu-Co nanorods doped with α-MnO_2. The successful incorporation of cobalt and copper was anticipated using X-ray diffraction. The average particle size of dual doped α-MnO_2 nanoparticles was estimated using XRD analysis. The functional group analysis was evaluated using FTIR Spectroscopy.

This co-precipitation approach provides advantages such as a simple and speedy preparative method, as well as easy control of particle size and composition, making it commercially frequently utilized due to its cost effectiveness. MnO_2 is one of the most popular catalysis materials because to its unique qualities such as high activity, low cost, low toxicity, and environmental compatibility.

Keywords: Dual doped α-MnO_2, XRD, Nanorods

Introduction:

Nanotechnology is the study and technology of materials with at least one of three dimensions less than one hundred nanometers. [1] Particles are important in study because of their distinct optical, structural, and magnetic properties. Several factors determine nanoparticle properties, including shape, size, composition, and structure [2]. Nanoparticle size is determined by their dimension and form, resulting in materials with consistent properties. Nanoparticle formation is dependent on a regulated core structure and size [3, 4]. Metal nanoparticles having a significant specific surface area have been extensively studied due to their distinct physical and electrical properties [5]. Manganese oxide nanoparticles have good physicochemical properties and can be employed in a wide range of applications, including catalysts, molecular sieves, batteries, magnetic materials, and more. The optical and electrical properties of produced manganese oxide nanoparticles are important aspects to consider for future research in solar cells [6].

Transition metal oxide nanostructures have emerged as a viable electrode material for energy storage [7]. Manganese is a transition element with three different valence states, and its oxides are regarded very complicated [8]. Among the transition metal oxides, manganese exhibits multiple oxidation states and hence forms distinct oxides (MnO, Mn_2O_3, Mn_3O_4, Mn_5O_8, and MnO_2) [9]. Nanoparticles, due to their large surface area, can perform both Faradic and Non-Faradaic charge transfer mechanisms. Kumar et al. and Balamurugan generated nanocrystalline manganese oxide nanoparticles with tetragonal structure via co-precipitation with two distinct anions salts (sulphate monohydrate and oxalate) [10, 11]. Wu et al. found that hydrothermal synthesis could generate many morphologies of MnO_2 nanostructures, including α-MnO_2 nanorods, nanotubes, and nanowires [12]. In this regard, manganese oxide (MnO_2) with its tetragonal structure and (2x2) tunnelled type Hollandite (alpha) network makes it a promising option for supercapacitor applications [13]. α-MnO_2 is most relevant due to its great chemical stability and long cycle life when used in electrochemical capacitors. [14].

Co oxidation was also observed on copper and manganese oxide, with the presence of Cu^{2+} and Mn^{3+} [15] Copper doped MnO_2 is the insertion of copper ions (Cu^{2+}) into the crystal structure of MnO_2. This doping procedure involves replacing some of the Mn atoms. With Cu atoms, changing the composition and characteristics of MnO_2. Copper doping can improve total conductivity by enabling charge transport inside the crystal lattice [16]. Cobalt is thought to be one of the most promising metal cations. Cobalt was discovered to be one of the most promising metal cations. Incorporating Co ions into MnO_2 produces a greater pseudo capacitance of cobalt oxide. Co-doped MnO_2 nanoparticles show a significant increase in electrode conductivity, and studies based on Co-MnO_2 suggest that it could be a viable electrode material for several high capacitive applications. [17] MnO_2 has various structural forms, including α, β, γ, δ, ε, and λ. The fundamental structural unit (MnO_6 Octahedron) is linked in various ways. [18]

MnO_2 nanoparticles can be prepared using either top-down or bottom-up processes. The top-down technique is not commonly used due to the high preparation cost and structural defects in the generated nanoparticles [19]. Most researchers prefer the bottom-up technique, which produces particles of homogeneous size and morphology. The wet chemical method is utilized to synthesize MnO_2 nanoparticles. This study focuses on summarizing the most commonly used wet chemical procedures, including hydrothermal [20], redox process [21], sol gel method [22], thermal reflex process [23], chemical precipitation method [24], and green synthesis method [25].

2. Experimental part

2.1. Chemical

The chemicals Manganese chloride tetrahydrate ($MnCl_2.4H_2O$), copper nitrate trihydrate ($Cu(NO_3)_2.3H_2O$), cobalt nitrate hexahydrate ($Co(NO_3)_2.6H_2O$) and sodium hydroxide (NaOH) were used the raw materials.

2.2. Synthesis of pure and dual doped α-MnO_2 nanorods

For the synthesis of dual doped α-MnO_2 nanorods, 0.98 g of $MnCl_2.4H_2O$ was dissolved in a beaker containing 50 ml of distilled water under ambient temperature. Then, 0.14 g of $Cu(NO_3)_2.3H_2O$ prepared in 20 ml aqueous was mixed with the above solutions drop by drop under a magnetic stirrer for 20 mins. Further, $Co(NO_3)_2.6H_2O$ of preferred molar ratios like 0.01, 0.02, 0.03, and 0.04 M prepared in 20 ml aqueous were mixed drop by drop. Finally, 0.2M of NaOH pellets were added and poured into the above solution till the pH value reached ~9. The entire solution was continuously agitated for 2 hrs and heated

at 80°C. To remove contaminants, the precipitate was washed multiple times with distilled water and ethanol after being filtered. The obtained final product was dried in hot air oven for 6 hours at 60°C and samples were subsequently calcinated at 450°C for 7 hrs. The annealed powders were pulverized into fine particles using an agate mortar for further characterization.

3. Characterization techniques

The structural properties of prepared pure and dual doped α-MnO_2 nanorods was studied by X-ray diffraction technique using Philips powder diffractometer (1729 PW) equipped with a monochromatic CuKα radiation source (λ=1.5406Å) for 2θ varying from 20°-60°. The FTIR spectroscopy with the Thermo Nicolet 380 equipment was used to investigate the vibrational bands of synthesized materials.

Results and discussion

3.1. Structural analysis

The structural analysis of pure and α-$MnO_{2(0.95-x)}$ $Cu^{2+}{}_{(0.05)}$ $Co_{(x)}$ nanorods with different concentration levels of cobalt doping (x= 0.01, 0.02, 0.03 and 0.04 M) are displayed in Fig. 1. The observed diffraction peaks are widened and high intensity suggested that prepared samples are well crystalline in nature. Also, the XRD spectra of all diffraction peaks were well accordance with the tetragonal crystal structure (JCPDS card no. 41-0141). The pure sample showed the diffraction peaks were related to the characteristic peaks of α-MnO_2 nanorods [26]. The characteristic peaks intensity was increased with increasing Co concentration upto 0.03M. The observed diffraction peaks located at 18.08°, 28.74°, 36.58°, 37.72°, and 49.90°, corresponding to the (220), (310), (400), (211) and (411) planes, respectively. These results indicated that the Co doped samples did not alter the crystal structure of α-MnO_2:Cu nanoparticles at lower concentrations. The lack of secondary peaks demonstrated the successfully incorporation of Co^{2+} ions into the host lattice, where they occupied Mn^{2+} without disrupting the tetragonal structure. Additionally, no characteristic peaks of cobalt oxide or cobalt hydroxide were observed up to 0.03M Co incorporation, which revealed that the dopant is well integrated into the lattice site during the preparation process. Further, the Co concentration was slightly raised to 0.04M, and the diffraction peaks intensity decreased.

The Debye-Scherrer's formula was used to evaluate the crystallite size of prepared samples [27].

$$D = \frac{k\lambda}{\beta \cos\theta} \quad (1)$$

where, λ was wavelength of the X-ray (λ=1.5406 Å), θ was the angle of the diffraction, k was shape factor, and β was full width half maxima of the peak. According from the Table. 1 indicated that the crystallite size of the dual doped α-MnO_2 nanorods decreased from 18 to 10 nm with increasing Co concentrations. The decreased crystallite size with increasing Co concentrations due to the observed diffraction peaks was broader. Also, the lattice constant was significantly raised when dual doped into the α-MnO_2 crystal structure, which results in lattice distortion and a further decreased crystallite size.

The lattice constant of the synthesized samples were estimated using the equation [28],

$$a = \frac{\lambda\sqrt{h^2+k^2+l^2}}{2\,Sin\theta} \quad (2)$$

where, hkl is the miller indices of the crystal and d is interplanar spacing. The estimated values for lattice constant were observed to be in the range of (*a*) 9.772–9.787 and *(c)* 2.853-2.866 Å for pure and dual doped α-MnO_2 nanorods, respectively. A small variation was observed in the lattice constant values with an increase in the Co^{2+} ratio, and it was in reasonable agreement with the JCPDS values.

The dislocation density and microstrain of pure and dual doped α-MnO_2 samples were determined by following the formulae [29,30],

$$\delta = \frac{1}{D^2} \quad (3)$$

$$(\varepsilon) = \frac{\beta}{4\tan\theta} \quad (4)$$

The dislocation density values increased with raising Co content attributed to decreased crystallite size. The calculated strain values increased with increased Co ratio due to the radius of Co^{2+} ions is significantly higher than that of Mn^{2+} ions, resulting in system instability.

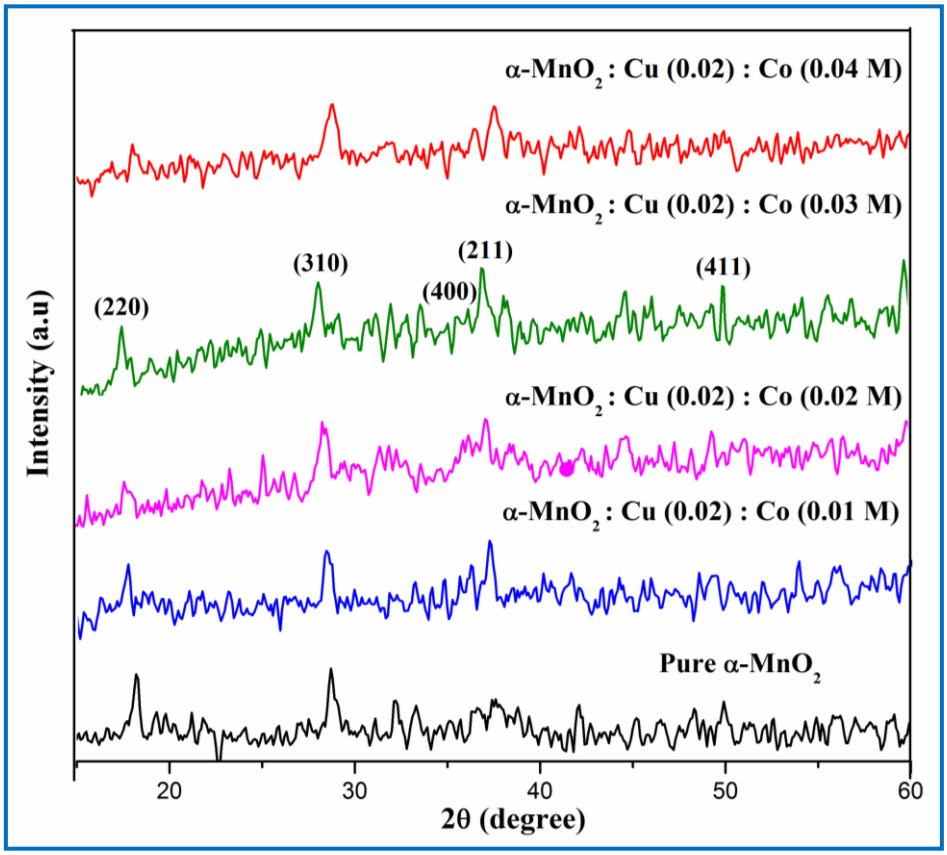

Fig. 1. XRD pattern of pure and dual doped α- MnO_2 nanorods.

Table 1. The structural parameters for dual Cu-Co doped α-MnO_2 nanoparticles.

Samples	Crystallite size (D) nm	Dislocation density (δ) x 10^{15} (lines/m^2)	Micro strain (ε)	Lattice constant (a) Å	
				a	*c*
Pure α-MnO_2	18	3.0864	0.5087	9.772	2.853
α-MnO_2:Cu(0.02M) :Co(0.01M)	15	4.4450	0.7906	9.776	2.855
α-MnO_2:Cu(0.02M) :Co(0.02M)	13	5.9172	0.8214	9.781	2.860

α-MnO_2:Cu(0.02M) :Co(0.03M)	12	6.9445	0.8472	9.784	2.865
α-MnO_2:Cu(0.02M) :Co(0.04M)	10	10.0012	1.0245	9.787	2.866

3.2. FTIR analysis

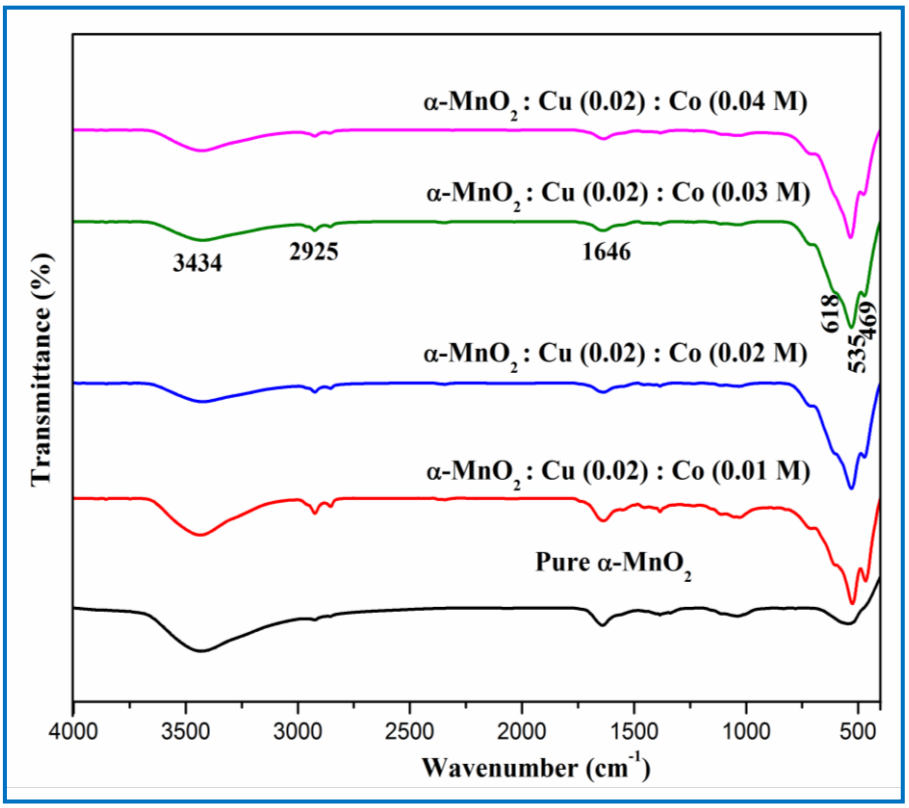

Fig. 2. FTIR spectra of pure and dual doped α-MnO_2 nanorods.

The molecular vibration characteristics of the α-MnO_2 nanorods with varying structures were investigated by recording FT-IR spectra. Fig. 2 displays the absorption bands measured in the range of 400–800 cm^{-1} were caused by the vibrations of Mn–O and Mn–O–Mn, which were clearly observed in the spectra of all four samples. The stretching vibration of the H_2O molecule and OH− in the lattice was responsible for the broad peak at 3434 cm^{-1}. The Co^{2+} and Cu^{2+} dual doped α-MnO_2 nanorods exhibited the strongest stretching vibration, while the OH−/H_2O stretching peak of the α-MnO_2 nanorods was nearly impossible to distinguish [31,32]. The phenomena can be attributed to the direct binding of hydroxyl groups and interlayer hydrates to the intercalated metal ions in the interlayer. The absorption band detected at 1646 cm^{-1} which is due to bending vibration. Also, the small absorption band detected at 2925 cm^{-1} can be attributed to the C-H stretching mode [33]. Compared to pure α-MnO_2 sample, dual doped samples intensity decreases along with characteristic peaks were shifted in lower angel side. The aforementioned phenomenon indicates that the phase of α-MnO_2 varies with metal intercalation, and the structure change was activated in a different content or manner by Co^{2+} and Cu^{2+} due to their varying valence and doping amounts. The XRD results were further confirmed by the FTIR results, which showed that no impurity phase was observed.

4. Conclusion

α-MnO_2 nanorods. Co-Cu-doped MnO_2 nanorods were produced using chemical precipitation and examined for structural and functional groups. Structural investigation revealed the tetragonal structure of α-MnO_2, supporting XRD findings at all Co concentrations. We successfully developed an electrode material for supercapacitor applications that utilizes pure and cobalt-copper dual doped Nanorod-like structures were seen in both pure and dual-doped α-MnO_2 samples. The length/diameter of the nanorods decreased as Co concentration increased.

References

1. T. Mounika, K. Meenu, S.L. Belagali, C. Dharmashekar, K.T. Vadiraj, C.Shivamallu, S.P. Kollur, Ferric oxide quantum dots (FOQDs) for photovoltaicand biological applications: Synthesis and characterization, Inorg Chem Commun 140, (2022) 109487
2. L. Ji, X. Zhang, Evaluation of Si/carbon composite nanofiber-based insertion anodes for new-generation rechargeable lithium-ion batteries, Energy Environ.Sci 3 , (2010) 124–129.
3. L. Qie, W.-M. Chen, Z.-H. Wang, Q.-G. Shao, X. Li, L.-X. Yuan, X.-L. Hu, W.-X.Zhang, Y.H. Huang, Nitrogen-Doped Porous Carbon Nanofiber Webs as Anodesfor Lithium Ion Batteries with a Superhigh Capacity and Rate Capability, Adv Mater 24 (15) , (2012) 2047–2050.
4. M. Jayandran, M. Muhamed Haneefa, V. Balasubramanian, Green synthesis and characterization of Manganese nanoparticles using natural plant extracts and its evaluation of antimicrobial activity, J Appl Pharm Sci 5,: (2015) 105–110.
5. R.N. Reddy, R.G. Reddy, Synthesis and electrochemical characterization of amorphous MnO_2 electrochemical capacitor electrode material, J Power Sources 132 , (2004) 315–320.
6. S. Mitra, Y. Pak, N. Alaal, M.N. Hedhili, D.R. Almalawi, N. Alwadai, K.Loganathan, Y. Kumarasan, N. Lim, G.Y. Jung, I.S. Roqan, Novel P-Type Wide Bandgap Manganese Oxide Quantum Dots Operating at Deep UV Range for Optoelectronic Devices, Adv Opt Mater 7 (21) (2019), 1900801.
7. K.D Sattler, Handbook of Nanophysics, Principles and methods (CRC,Newyork) (2010)
8. Zhen-Yu Li , M. Shaheer Akhtar , Phuong T.M. Bui , O-Bong Yang, Predominance of 2D Mn_2O_3 nanowalls thin film for high performance electrochemical supercapacitors. Chemical Engineering Journal , Volume 330, (2017) , Pages 1240-1247.
9. H.Adelkhni , M.Ghaemi and S.M.jafari, Novel nanostctured MnO_2 Prepared by pulse electrodeposition; characterization and electro kinetics , J.Mater .Sci.Technol.,(2018) Vol.24 no.6.
10. H.K. Manisha and P. Sangwan, “Synthesis and Characterization of MnO_2 Nanoparticlesusing co precipitation Technique,” International Journal of chemistry and Chemical Engineering,Vol.3, Number 3, (2013) pp. 155-160.
11. M. Balamurugan, G. Venkatesan, S. Ramachandran and S. Saravanan, “Synthesis and Characterization of Manganese Oxide Nanoparticles,” Synthesis and Fabrication of Nanomaterials, (2015) pp. 311-314.
12. Wen Yao, Yihan Wu, Hongwei Pang, Xiangxue Wang, Shujun Yu & Xiangke Wang. *In-situ* reduction synthesis of manganese dioxide@polypyrrole core/shell nanomaterial for highly efficient enrichment of U(VI) and Eu(III), Volume 61, (2018) pages 812-823 Articlesblished: 15 March 2018
13. D. Mondal, et al, "Size engineered Cu-doped α-MnO_2 nanoparticles for exaggerated photocatalytic activity and energy storage application" Materials Research Bulletin 115 (2019) 159–169.

14. Nobuhiro Shimamura, Ryuji Kanda, Yuma Matsukubo,Yutaro Hirai,Hiroya Abe,Yuj Hirai,Tsukasa Yoshida, Hiroshi Yabu, and Akito Masuhara, "Preparation of Hierarchi Porous Films of α-MnO_2 Nanoparticles by Using the Breath Figure Technique and Application for Hybrid Capacitor Electrodes", ACS Omega 4, (2019) 3827-3831
15. M. Krämer, T. Schmidt, K. Stöwe, W. Maier, Structural and catalytic aspects of sol–gederived copper manganese oxides as low-temperature CO oxidation catalyst App. Catal. A 302 , (2006) 257–263 .
16. Rong Lan,Evangelos Gkanas, Ali Jawad Sahib Sahib, Agata Greszta, Rohit Bhagat, Alexander Roberts, The effect of copper doping in α-MnO_2 as cathode material fo aqueous Zinc-ion batteries, Journal of Alloys and Compounds Volume 992, (2024) 174528
17. S.Sivakumar, Nelson Prabu "Enhancement in Electrochemical behavior of Cobalt doped α- MnO_2 Nanoparticles. Inorganic chemistry communication , Volume 147, (2023) 110247.
18. Y.chen,Y.Hong,Y.Ma and j.LI, "Synthesis and formation mechanism of urchin like nano/micro hybrid α-MnO_2" Journal of Alloys and compounds. Vol.490.(2002) p.p.2880-2881
19. Nikam A , Prasad B L and Kulkarni A , Wet chemical synthesis of metal oxide nanoparticles: a review Cryst Eng Comm 20 , (2018) 5091.
20. Qi S Y, Feng J, Yan J, Hou X Y and Zhang M L Chin. J. Manganese dioxide nanoparticles Synthesis, application and challenges Nonferrous Met. (2008) 18 113 .
21. Zhang H T, Chen X H, Zhang J H, Wang G Y, Zhang S Y, Long Y Z et al , Synthesis and characterization of one-dimensional $K_{0.27}MnO_2 \cdot 0.5H_2O$,J. Cryst. Growth (2005) 280 292.
22. Ching S, Roark J L, Duan N and Suib S L, Sol−Gel Route to the Tunneled Manganese Oxide Cryptomelane, (1997) Chem. Mater. 9 750
23. Yin H, Dai X, Zhu M, Li F, Feng X and Liu F , J. Fe-doped cryptomelane synthesized by refluxing at atmosphere: Structure, properties and photocatalytic degradation of phenol (2015) Hazard Mater. 296 22
24. Shaker K and Abdalsalm A H , Synthesis and Characterization Nano Structure of MnO2 via Chemical Method , Eng. Tech. J. 36 (2018) 946 .
25. Sinha A, Nand V, Raj B and Kumar S , Synthesis and characterization of monodispersed orthorhombic manganese oxide nanoparticles produced by Bacillus sp cells simultaneous to its bioremediation J. Hazard. Mater. (2011) 192 620
26. Sarika M. Jadhav, Ramchandra S. Kalubarme, Norihiro Suzuki, Chiaki Terashima, Junyoung Mun, Bharat Bhanudas Kale, Suresh W. Gosavi, Akira Fujishima, Cobalt-DopedManganese Dioxide Hierarchical Nanostructures for Enhancing Pseudocapacitive Properties, ACS Omega, 6 (2021) 5717-5729.
27. Muhammad Touqeer, Mirza Mahmood Baig, Muhammad Aadil, Philips O. Agboola, Imran Shakir, Mohamed F. Aly Aboud, Muhammad Farooq Warsi, New Co-Mn based Nanocrsytallite for photocatalysis studies driven by visible light, Journal of Taibah University for Science, 14(1) , (2020) 1580-1589 .
28. M. Shakir, S.K. Kushwaha, K.K. Maurya, G. Bhagavannarayana, M.A. Wahab, Characterization of ZnSe nanoparticles synthesized by microwave heating process Solid State Commun. 149 (45–46) (2009) 2047–2049.

29. M. Shkir, Noticeable impact of Er doping on structural, vibrational, optical, dielectric and electrical parameters of flash combustion synthesized NiO NPs for optoelectronic applications, Inorg. Chem. Commun. 121 , (2020) 108229 .
30. M. Shkir, Enhancement in optical and electrical properties of ZnO thin films via C doping for photodetector applications, Mater. Sci. Eng. B 284 (2022), 115861.
31. S. Karpagavalli, S. John, S. Perumal, P. Koilpillai, A. Suganthi, A comparative study of optical and magnetic properties of undoped and cobalt doped manganese oxid nano particles, IOSR J. Appl. Phys. (2017) 34–42 .
32. Y. Kumar, Seema Chopra, A. Gupta, Y. Kumar, S.J. Uke, S.P. Mardikar, Low temperature synthesis of MnO2 nanostructures for supercapacitor application, Mater. Sci.Energy Technol. 3 , (2020) 566–574 .
33. Chadia Belkhaoui, Nissaf Mzabi, Hichem Smaoui, Investigations on structural, optical and dielectric properties of Mn doped ZnO nanoparticles synthesized by co-precipitation method, Materials Research Bulletin, 111, (2019) Pages 70-79.